ELSEVIER

International Journal of Heat and Fluid Flow 21 (2000) 554–561

International Journal of HEAT AND FLUID FLOW

www.elsevier.com/locate/ijhff

Effect of inter-particle spacing on turbulence modulation by Lagrangian PIV

Yohei Sato [a,*], Ushio Fukuichi [b,1], Koichi Hishida [b,1]

[a] *Fluid Engineering Division, Department of Energy Engineering, Mechanical Engineering Laboratory, AIST, MITI, 1-2 Namiki, Tsukuba Science City, Ibaraki 305-8564, Japan*

[b] *Department of System Design Engineering, Faculty of Science and Technology, Keio University, 3-14-1 Hiyoshi, Kohoku-ku, Yokohama 223-8522, Japan*

Abstract

Turbulence modulation by solid particles in a fully developed channel flow was investigated by Lagrangian measurement technique. Digital particle image velocimetry (DPIV) and a high-speed CCD camera mounted on a shuttle moving with particle mean streamwise velocity were used to simultaneously detect particle and fluid information among particles. Two classes of particles at particle volumetric fraction up to 3.32×10^{-4} were employed to provide characteristic values of length ratio and distance between particles, i.e., inter-particle spacing. Turbulence augmentation by particles greater than the Kolmogorov micro-length-scale was induced by a region of high strain rate and high vorticity located on both sides of the particles. The rapid distortion theory (RDT) applied to dispersed two-phase turbulent flows substantiates the observed directional non-isotropic structure with an increase in particle volumetric fraction. The enstrophy production was enhanced with decreasing values of inter-particle spacing, yielding an increase in the enstrophy among particles.

Keywords: Dispersed two-phase flows; Lagrangian PIV; Inter-particle spacing; Turbulence distortion; RDT; Directional interaction

1. Introduction

One of the most important aspects of dispersed two-phase flows is the interactions of solid particles or liquid droplets with turbulent flow fields. In fact the performance of many engineering devices, as well as natural processes encompass dispersed two-phase flows. An increased understanding of the fundamental phenomena, that drive the complex interactions between the particle cloud and turbulent carrier flow, is needed to ultimately improve the design of engineering devices in which these flows occur. The available experimental data show that the addition of small particles suppresses turbulent kinetic energy, while large particles increase turbulence (Tsuji and Morikawa, 1982; Tsuji et al., 1984; Fleckhaus et al., 1987; Rogers and Eaton, 1991; Kulick et al., 1994; Sato et al., 1996). While the works using direct numerical simulation by Squires and Eaton (1990), Elghobashi and Truesdell (1993), and Boivin et al. (1998) have advanced our understanding, the effect of particles on turbulence modulation is not fully resolved up to this day.

To date the macro-scale analyses present the following consensus interpretation. Gore and Crowe (1989a,b) compiled data, foremost expressing the ratio of particle diameter to a characteristic length-scale of the turbulence as a key parameter. They suggested that the critical value of the ratio separating regions of attenuation and augmentation was on the order of 0.1. Eaton (1994) reviewed past experiments and simulations in turbulence modification of simple flows and showed significant turbulence attenuation for mass-loading ratios greater than 0.1. Sato and Hishida (1996) introduced the multiple time-scale concept to more accurately model the energy transport due to particles from the production range to the transfer range of the fluid velocity spectrum. An outcome of these works revealed that the particle size and loading have a significant influence on turbulence modification. However, experimental findings on turbulence distortion among particles do not exist, thus the small-scale structure of turbulence in the vicinity of particles is not clearly known.

The objective of this study is to investigate the turbulence distortion process in the presence of particles in a turbulent channel flow via Lagrangian measurement established by Sato et al. (1997). A non-uniform distortion of turbulence among particles was first detected by digital particle image velocimetry (DPIV) (Sakakibara et al., 1993) using a high-speed CCD camera mounted on a shuttle moving with particle streamwise mean velocity. Crowe and Gillandt (1998), and Crowe (1998) recently proposed an inclusion of inter-particle

* Corresponding author. Tel.: +81-298-61-7243; fax: +81-298-61-7091.

E-mail address: yohei@mel.go.jp (Y. Sato).

[1] Tel.: +81-45-566-1739; fax: +81-45-566-1720.

0142-727X/00/$ - see front matter
PII: S0142-727X(00)00044-8

Notation

d_p particle diameter
h channel width
k turbulent kinetic energy
l_e length-scale of energy-containing eddies ($= k^{3/2}/\varepsilon$, ε: dissipation rate of k)
l_p inter-particle spacing
Re_h channel Reynolds number
Re_p particle Reynolds number
$s_{ij}^{p>}$ rate of strain *seen by particle*
t time
$u_f^{p>}$ streamwise fluctuating fluid velocity *seen by particle*
$\langle U_c \rangle$ streamwise mean velocity of water at channel centerline in single-phase
$\langle U_f \rangle$ streamwise mean velocity of water in the Eulerian reference frame
$v_f^{p>}$ transverse fluctuating fluid velocity *seen by particle*
V_t particle terminal velocity ($= \tau_p g$, g: gravity)
x, y Cartesian coordinate system in the Eulerian reference frame
x^C, y^C Cartesian coordinate system located on a high-speed CCD camera

Greeks
η Kolmogorov micro-length-scale
ν kinematic viscosity of water
ρ density
σ_p standard deviation of diameter
$\Sigma^{p>}$ RDT parameter
τ_K Kolmogorov micro-time-scale
τ_p particle time constant
ϕ_{mass} particle mass-loading ratio
ϕ_{vol} particle volumetric fraction
$(\omega_i^{p>})^2$ enstrophy *seen by particle*
$\omega_{ij}^{p>}$ vorticity *seen by particle*

Subscripts
f fluid property
i ith component
j jth component
p particle property

Superscripts
$p_>$ property *seen by particle*

spacing into the model of the dissipation rate. They pointed out that the dissipation term depends on the local gradients and the inter-particle spacing. None of the experiments, however, investigated an influence of the inter-particle spacing on the distortion of turbulence. Therefore, the present study focuses on the turbulence distorted by particles in terms of the inter-particle spacing and investigates the small-scale structure of turbulence modulation by particles from the experimental point of view.

2. Experimental setup

2.1. Experimental facility

The present experiments were performed in a two-dimensional, vertical channel with downflow of water, identical to that of Sato et al. (1997). The channel was vertically oriented, so that the gravitational force on the particles was aligned with the direction of flow. The particle feeder was mounted above the entrance of the channel. The particle loading uniformity was ensured by vibrating the particle feeder with a DC-motor. Boundary layer trips were affixed to both walls at the entrance to a 1.0 m long, 30×250 mm test section. The flow exited the test section into a drain tank, where the particles were collected for reuse. Measurements confirmed that the flow was fully developed at the test section's centerline. Some of the properties of the flow are presented in Table 1. All the experiments were run at a centerline mean velocity of 155 mm/s, corresponding to a Reynolds number of 5740 based on channel width. The temperature of water was kept constant by using a heater to avoid varying fluid properties. The Kolmogorov micro-length and time-scales were calculated by direct measurements of dissipation rate of turbulent kinetic energy.

Two classes of particles were used in the present set of experiments and their characteristics are compiled in Table 2. The particle size was chosen with the following strategy: (i) smaller than the energy-containing scales of the flow; (ii) comparable to or slightly greater than the Kolmogorov micro-length-scale of turbulence. The particle size distributions were determined by using successively smaller sieves, while the particle sphericity was checked by using a microscope.

Table 1
Fluid flow parameters

Channel width, h (mm)	30
Centerline mean velocity, $\langle U_c \rangle$ (mm/s)	155
Channel Reynolds number, Re_h	5740
Kinematic viscosity of water, ν (mm^2/s)	0.810
Kolmogorov micro length scale[a], η (μm)	252
Kolmogorov micro time scale[a], τ_K (ms)	78.4

[a] Value at channel centerline.

2.2. Experimental techniques

Velocities of both phases were obtained by using a DPIV method developed by Sakakibara et al. (1993), and Sato et al. (1995, 1997). Fig. 1 shows a schematic illustration of the DPIV. The illuminated laser light sheet was chopped by an acoustic optical modulator (AOM) cell for synchronizing to the timing controller. Velocities were calculated by a cross-correlation technique between two images. Polyethylene particles of 5 μm (density of 960 kg/m^3) were added as a tracer to the liquid phase. The thickness of the YAG-laser light sheet was 3.0 mm in the test section.

A high-speed CCD camera (KODAK Motion Corder Analyzer SR-500) and a cylindrical lens were mounted on a moving shuttle in order to establish the Lagrangian measurement technique. The present measurement system simultaneously detected particles and fluid information. The shuttle moved from top to bottom, parallel to the water channel, with mean streamwise velocity of the particles upon which it focuses. A stepping motor was used to control the shuttle's velocity and calibration to account for the influence of vibration of the shuttle velocity was conducted. A special calibration scale in which solid marks were randomly distributed as if particle concentration were detected, as shown in Fig. 1(a), was added to the present system (Sato et al., 1997). The CCD camera captured the images of the flow field in the test section

Table 2
Particle properties

Properties	Glass	Glass	Glass
Number mean diameter, d_p (μm)	189.5	396.4	396.4
Standard deviation of diameter, σ_p (μm)	18.0	32.3	32.3
Density, ρ_p (kg/m^3)	2590	2590	2590
Terminal velocity, V_t (mm/s)	43.1	102	102
Particle time constant, τ_p (ms)	4.40	10.4	10.4
Particle Reynolds number[a], Re_p	10.1	50.0	50.0
Particle mass loading ratio, ϕ_{mass}	4.10×10^{-4}	3.32×10^{-4}	8.63×10^{-4}
Particle volumetric fraction[b], ϕ_{vol}	1.77×10^{-4}	1.80×10^{-4}	3.32×10^{-4}

[a] Mean value calculated using instantaneous particle Reynolds number.
[b] Calculated using mean streamwise velocity shown in Fig. 2(a).

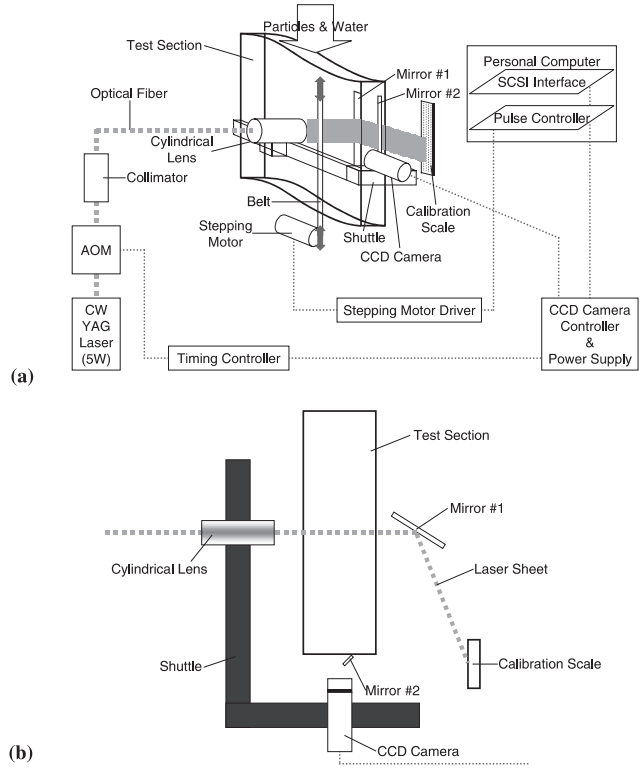

Fig. 1. Schematic of experimental apparatus: (a) schematic of DPIV and vertical water channel; (b) top view of experimental facility.

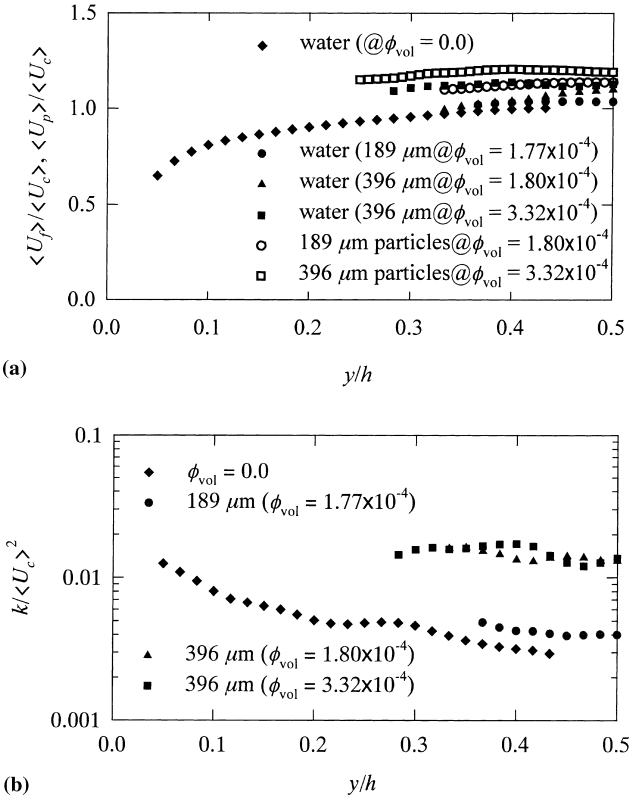

Fig. 2. Profiles of: (a) mean streamwise velocity of water and particles; (b) turbulent kinetic energy of water in the presence of particles.

and the calibration scale by using mirror #2, illuminated by a laser sheet via mirror #1, as illustrated in Fig. 1(b). Fig. 3(c) displays a representative time series of the instantaneous flow field and the calibration scale captured by the CCD camera. By using the DPIV system combined with the moving shuttle it is possible to calibrate the shuttle's vibration per unit image. The measurement uncertainty in these experiments due to the velocity calibration was 2.0% for instantaneous velocity measurements. The particles and surrounding fluid were measured by the high-speed CCD camera in a matter of few seconds. Subsequently, velocities in time series were calculated within an interval of 1/62.5 s (= 16 ms).

3. Results and discussion

3.1. Properties of the Eulerian field

Fig. 2 shows profiles of the mean streamwise velocity and turbulent kinetic energy of water in the presence of glass particles. The coordinates of the figure have non-dimensionalized values based on the centerline mean velocity in single phase, $\langle U_c \rangle$, of 155 mm/s and a channel width, h, of 30 mm. It is observed that the particle-laden mean fluid velocity was accelerated by only 396 μm glass particles at high particle volumetric fraction and all the particles augmented the turbulent kinetic energy. The degree of turbulence augmentation in the core region increases with increasing particle volumetric fraction. In the present paper, the distortion process by particles at the channel centerline is reported.

Ongoing research investigations conducted by the authors using a laser technique indicate that particles, comparable to or slightly greater than the Kolmogorov micro-length-scale of the flow with a large particle time constant, augment the turbulence energy, while particles smaller than the micro-scale attenuate the turbulence (compiled in Hishida and Sato, 1999). Sato and Hishida (1996), and Hishida and Sato (1999) then

concluded that the effect of particles on turbulence structure is dependent upon the scale of turbulent flow. Thus depending on this scale, one can propose a criterion to distinguish between turbulence attenuation or augmentation in the presence of particles. Their analyses were performed from a macroscopic point of view. Therefore a microscopically viewed investigation of the existing data has proven to be somewhat controversial. The discussions in the following subsections have been inspired by the idea of inter-particle spacing (Crowe and Gillandt, 1998; Crowe, 1998) and emphasize the turbulence distortion among particles.

3.2. Definition of properties seen by particle

A fluid flow is specified in the Eulerian way, while a Cartesian coordinate system is located on the high-speed CCD camera. The coordinate system moving with particle mean streamwise velocity is defined as (x^C, y^C), where only y^C is identical to y in the Eulerian reference frame. The fluctuating fluid velocity *seen by particle* in the streamwise and transverse direction is introduced, respectively, as $u_f^{p_>}$ and $v_f^{p_>}$, where the superscript $p_>$ stands for the turbulent property *seen by particle*. The rate of strain *seen by particle* is defined as

$$s_{12}^{p_>} = \frac{1}{2}\left(\frac{\partial u_f^{p_>}}{\partial y^C} + \frac{\partial v_f^{p_>}}{\partial x^C}\right) \tag{1}$$

and the vorticity *seen by particle* is calculated by the circulation around each grid point to avoid an error in derivative (Sakakibara et al., 1993);

$$\begin{aligned}\omega_{12}^{p_>} = (&-u_{f_{1,1}}^{p_>}\Delta x^C - u_{f_{0,1}}^{p_>}\Delta x^C - v_{f_{-1,1}}^{p_>}\Delta y^C - v_{f_{-1,0}}^{p_>}\Delta y^C \\ &+ u_{f_{-1,-1}}^{p_>}\Delta x^C + u_{f_{0,-1}}^{p_>}\Delta x^C + v_{f_{1,-1}}^{p_>}\Delta y^C \\ &+ v_{f_{1,0}}^{p_>}\Delta y^C)/(4\Delta x^C \Delta y^C)\end{aligned} \tag{2}$$

which was found to vary within ±3% based on the measurement uncertainty.

3.3. Distortion of turbulence among particles

To investigate the distortion process of fluid turbulence amongst particles, the time development of instantaneous maps of the rate of strain and the vorticiy *seen by particle* are illustrated in Figs. 3–5, and images of the flow field detected by the high-speed CCD camera are shown in Fig. 3(c). At a constant value of particle volumetric fraction, the rate of strain and the vorticity in the presence of 396 μm glass particles (Figs. 5(a) and (b)) show larger values than those in the presence of 189 μm particles (Figs. 4 (a) and (b)) as the complexity of flow structure increases. This effect becomes more apparent as particle volumetric fraction increases as shown in Figs. 3(a) and (b). It is observed in the presence of 396 μm particles at a volumetric fraction of 3.32×10^{-4} that decreasing values of distance between particles, i.e., inter-particle spacing, have a significant effect on the rate of strain and the vorticity, yielding augmentation of turbulent kinetic energy shown in Fig. 2(b). The inter-particle spacing in Figs. 3(a) and (b) have values of $l_p/\eta \approx 10$ and $l_p/l_e \approx 0.6$. This means that there are a few particles (a calculated value using experimental data shows 1.7) inside the energy-containing eddy, as the turbulence was augmented by particles greater than the Kolmogorov length-scale.

We can see that the regions of high strain rate contain large vorticity on both sides of the particle. We thus think it is likely that the directional interaction between the flow and a particle induces distortion of turbulence by the particles themselves. We believe this to be a new physically plausible argument based on the existing data sets.

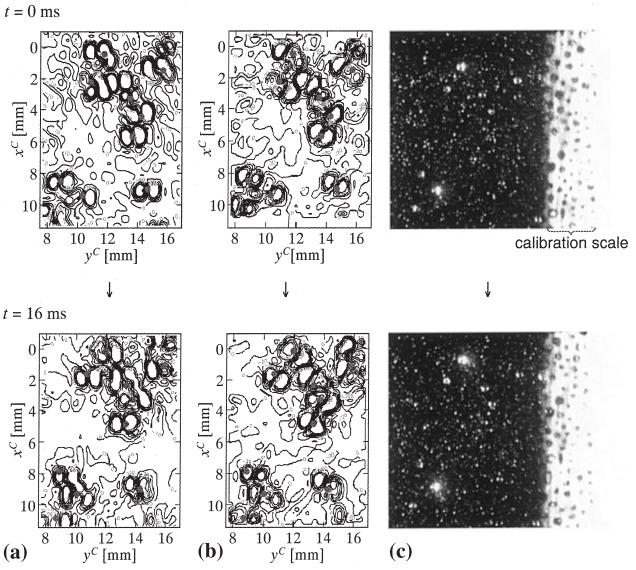

Fig. 3. Time development of instantaneous maps of: (a) the rate of strain, $s_{12}^{p_>}$; (b) the vorticity, $\omega_{12}^{p_>}$; (c) images of flow field in the presence of 396 μm glass particles at volumetric fraction of 3.32×10^{-4}. Range of $s_{12}^{p_>}$ is [−40, −30, −20, −10, 0, 10, 20, 30, 40] and $\omega_{12}^{p_>}$ is [−80, −60, −40, −20, 0, 20, 40, 60, 80].

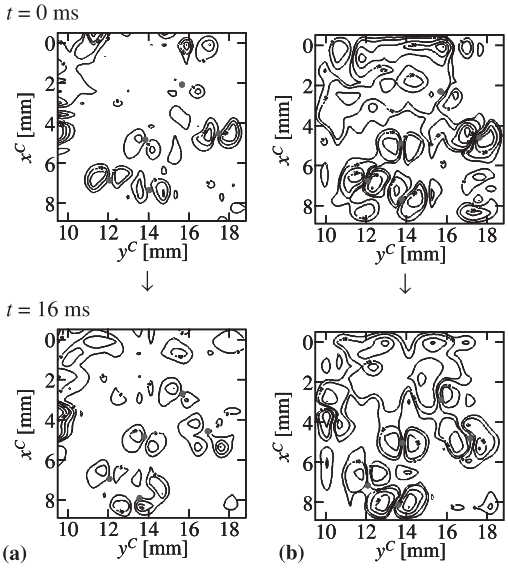

Fig. 4. Time development of instantaneous maps of: (a) the rate of strain, $s_{12}^{p_>}$; (b) the vorticity, $\omega_{12}^{p_>}$, in the presence of 189 μm glass particles at volumetric fraction of 1.77×10^{-4}. Range of $s_{12}^{p_>}$ is [−10, −5, 0, 5, 10] and $\omega_{12}^{p_>}$ is [−30, −20, −10, 0, 10, 20, 30].

3.4. Directional non-isotropic flow structure among particles based on the rapid distortion theory

Sato and Hishida (1996) first proposed an energy transfer mechanism from large to small-scale by particles. This is subsequently reflected in a multiple-time-scale model. The physical argument was that the large-scale structures determine the distortion experienced by small-scales and by the particles. In this subsection, the extent of this distortion is investigated using rapid distortion theory (RDT). The flow is divided into different structural types using an algorithm

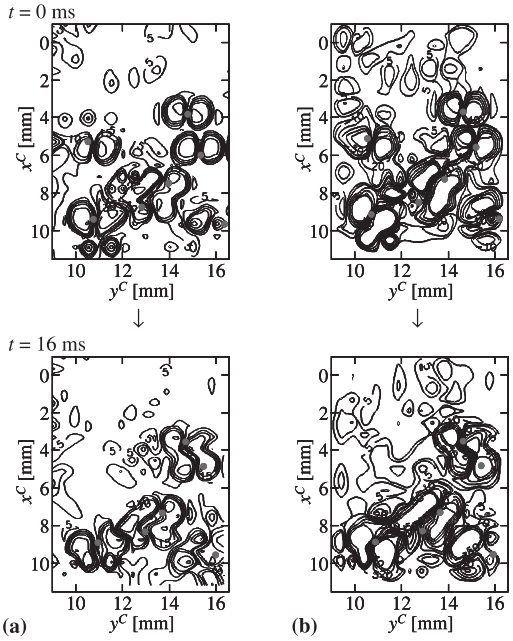

Fig. 5. Time development of instantaneous maps of: (a) the rate of strain, $s_{12}^{p>}$; (b) the vorticity, $\omega_{12}^{p>}$, in the presence of 396 μm glass particles at volumetric fraction of 1.80×10^{-4}. Range of $s_{12}^{p>}$ is [−10, −5, 0, 5, 10] and $\omega_{12}^{p>}$ is [−30, −20, −10, 0, 10, 20, 30].

developed by Kevlahan (1993), based on values of velocity and the parameter $\Sigma^{p>}$ defined as

$$\Sigma^{p>} = \frac{s_{ij}^{p2>} - \omega_{ij}^{p2>}}{s_{ij}^{p2>} + \omega_{ij}^{p2>}}, \tag{3}$$

where $s_{ij}^{p>}$ is the rate of strain tensor *seen by particle*, and $\omega_{ij}^{p>}$ is the vorticity tensor *seen by particle*. The four basic structural types are:

1. *Eddy*: $\Sigma^{p>} < -\frac{1}{3}$. Kevlahan (1993) used values of pressure, p, to distinguish between eddy ($p<0$) and donor eddies ($p>0$). However, in the present study it is impossible to measure fluctuating pressure using DPIV. Therefore, these two regions have been combined into one region. By using a threshold value of 1/3, we naturally focus on the flow structure in the region of the energy-containing eddy.
2. *Shear*: $-\frac{1}{3} \leqslant \Sigma^{p>} \leqslant \frac{1}{3}$.
3. *Convergence*: $\frac{1}{3} < \Sigma^{p>}$.
4. *Streaming*:

$$|u_{f_i}^{p>}| > \sqrt{\langle u_{f_i}^{p2>}\rangle}, \quad |\omega_{ij}^{p>}| > \sqrt{\langle \omega_{ij}^{p2>}\rangle}, \quad |s_{ij}^{p>}| > \sqrt{\langle s_{ij}^{p2>}\rangle}.$$

Fig. 6 shows the time development of instantaneous flow structure amongst particles based on RDT. With wide inter-particle spacing, as supported by Fig. 6(a) for 189 μm particles at $\phi_{vol} = 1.80 \times 10^{-4}$, the eddy region is noticeable, especially along both sides of several particles. The complexity of the flow structure evidently increases in Fig. 6(b), as particle size increases to 396 μm and then additionally as volumetric fraction increases, yielding narrow inter-particle spacing. One can see that a non-isotropic flow structure appears amongst particles in Fig. 6(c). It can be concluded that particles greater

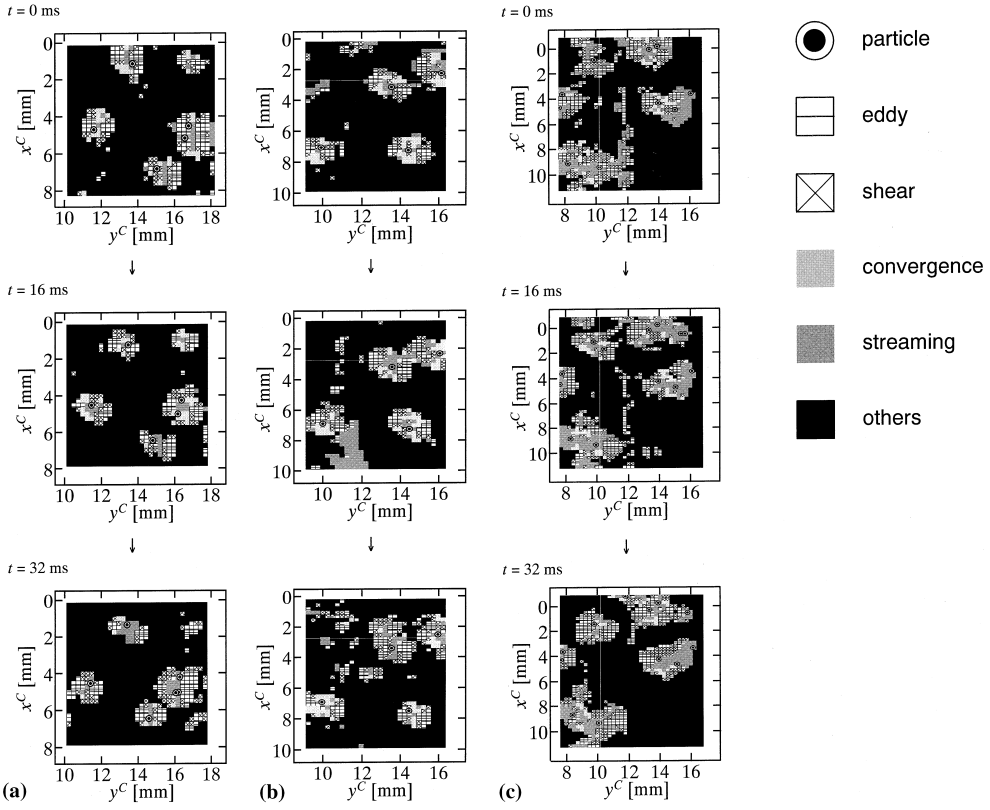

Fig. 6. Time development of non-isotropic flow structure in the presence of particles based on the RDT by Kevlahan (1993). (a) Glass 189 μm at $\phi_{vol} = 1.77 \times 10^{-4}$. (b) Glass 396 μm at $\phi_{vol} = 1.80 \times 10^{-4}$. (c) Glass 396 μm at $\phi_{vol} = 3.32 \times 10^{-4}$.

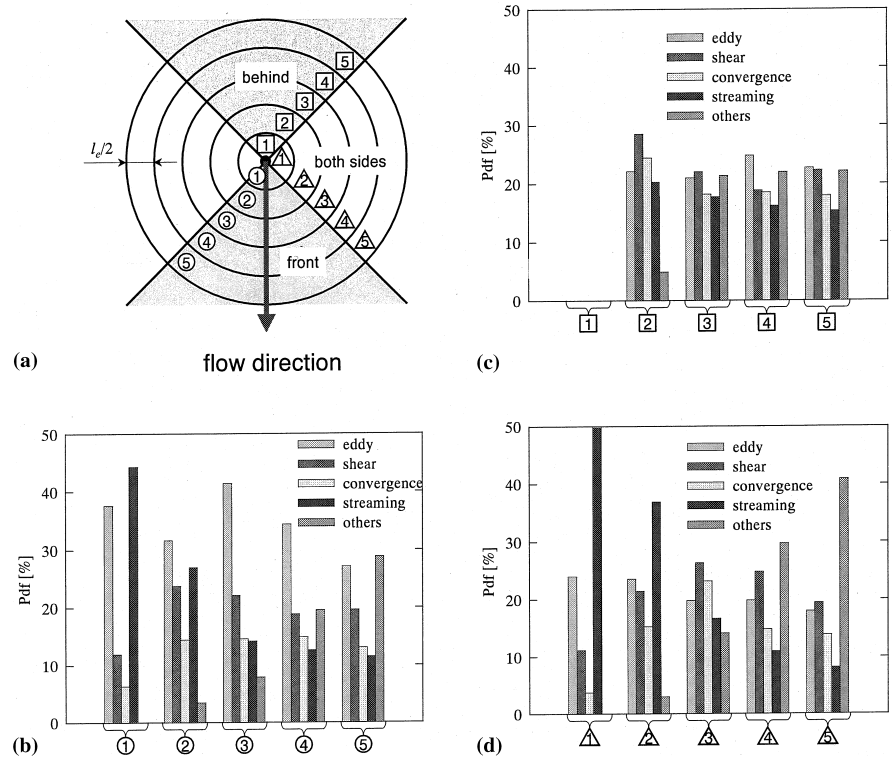

Fig. 7. (a) Schematic of regional classification around particle. (b) P.d.f. of structural types in front of 396 μm particle. (c) P.d.f. of structural types behind 396 μm particle. (d) P.d.f. of structural types along both sides of 396 μm particle. Particle volumetric fraction was 3.32×10^{-4}.

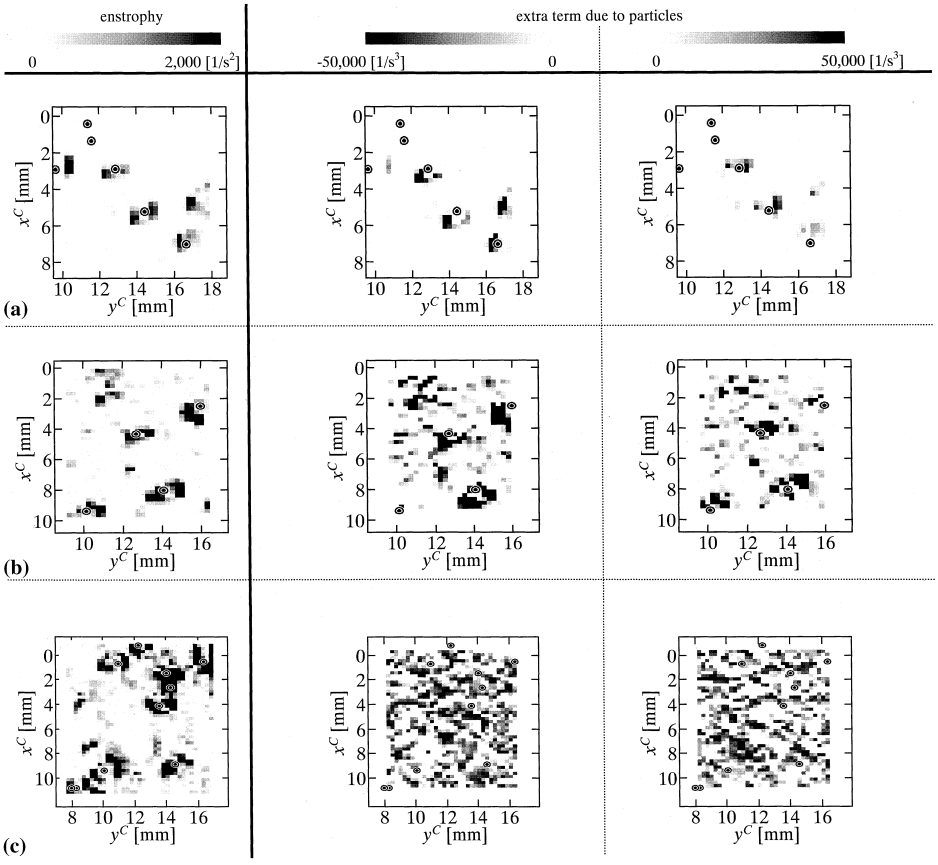

Fig. 8. Distribution of images of the enstrophy and the extra term due to particles in the enstrophy evolution equation in the presence of: (a) glass 189 μm at $\phi_{vol} = 1.77 \times 10^{-4}$; (b) glass 396 μm at $\phi_{vol} = 1.80 \times 10^{-4}$; (c) glass 396 μm at $\phi_{vol} = 3.32 \times 10^{-4}$. The enstrophy distribution has dimensional values in $1/s^2$, while the extra term due to particles has both positive and negative values in $1/s^3$.

than the Kolmogorov length-scale significantly distort the flow around particles, yielding a narrow inter-particle spacing and directional, non-isotropic and complex interaction of the flow structures.

Further insight into the directional interaction between particles and turbulence is provided by the probability density function (p.d.f.) of structural types around 396 μm particles as shown in Fig. 7. Fig. 7(a) indicates the schematic definition of regional classification, i.e., in front of, behind and along both sides of the particle. The abstraction of structural types in each sector was performed based on the length-scale of energy-containing eddies, i.e., $nl_e/2 < l_p < (n+1)l_e/2$. It is obvious from Fig. 7(c) that the structural types behind the particle are independent of the value of inter-particle spacing. On the other hand, one can see from Figs. 7(b) and (d) that different structural types appear in front of and along both sides of particle with increasing values of inter-particle spacing. This means that the direct effect of particles on fluid turbulence results in the directional interactions from the small-scale point of view.

3.5. Small-scale structure of turbulence modulation by particles

Since non-uniform distortion of turbulence is characterized by vortex structure, further insight into the small-scale structure of dispersed two-phase turbulent flow may be provided by the enstrophy, $(\omega_i^{p>})^2$, amongst particles *seen by particle*. In order to examine the small-scale structure, the enstrophy evolution equation is defined as

$$\frac{D}{Dt}\left\{\frac{1}{2}(\omega_i^{p>})^2\right\} = \omega_i^{p>}\omega_j^{p>}s_{ij}^{p>} + \nu\frac{\partial^2}{(\partial x_j^C)^2}\left\{\frac{1}{2}(\omega_i^{p>})^2\right\} - \nu\left(\frac{\partial\omega_i^{p>}}{\partial x_j^C}\right)^2 + (\text{extra term due to particles}), \tag{4}$$

where the terms on the right-hand side of Eq. (4) are the enstrophy production, which is due to vortex stretching, enstrophy diffusion, enstrophy dissipation and lastly an additional term due to particles. The fourth term was calculated by subtracting all the terms except the fourth term on the right-hand side from the left-hand side of the equation.

Fig. 8 depicts distribution of the enstrophy *seen by particle* and the extra term due to particles, the fourth term in Eq. (4), amongst particles. Values of the extra term have both positive and negative values, which are displayed in the left- and right-hand sides in Fig. 8, respectively. The enstrophy around a particle is larger as the inter-particle spacing becomes narrower. The positive values of the extra term adding the enstrophy can be found behind particle, while the negative values in front of particle. It is observed that the intensity of extra term is correlated with the value of inter-particle spacing.

Spatial distribution of all the terms except the extra term due to particles in the enstrophy evolution equation is illustrated in Fig. 9. The distribution has values of the ratio of each term to the left-hand side of Eq. (4). For 189 μm particles (Fig. 9(a)), the diffusion term has larger values than other terms. A concentration of enstrophy appears in the region,

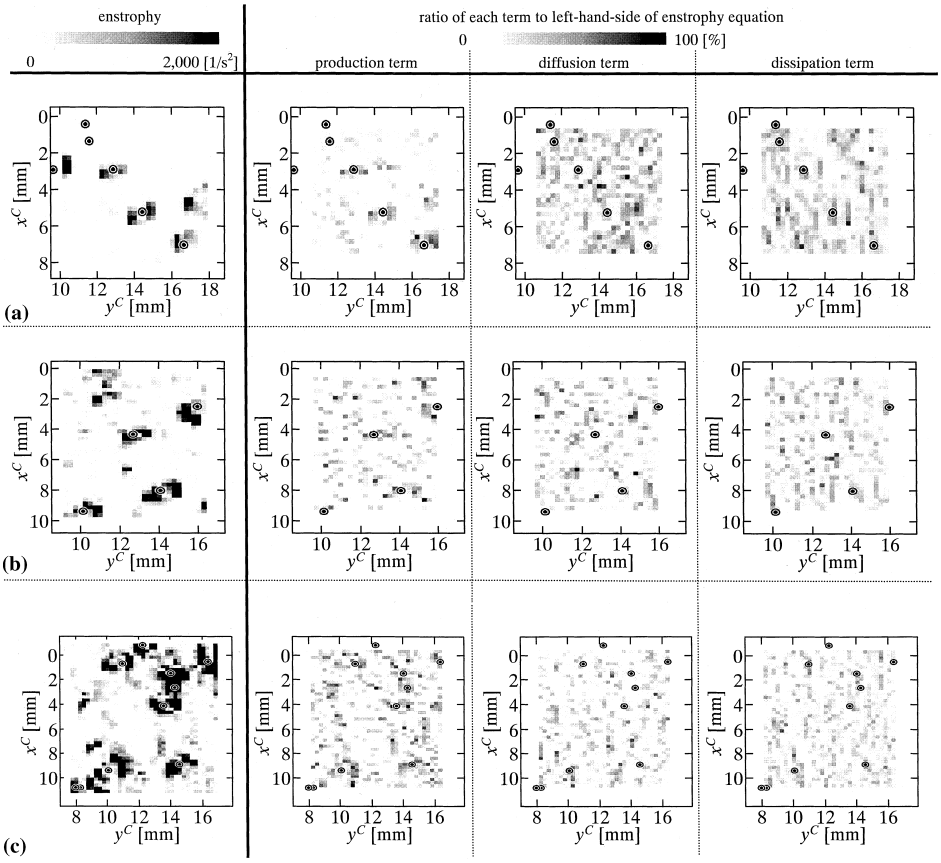

Fig. 9. Distribution of images of the enstrophy and each term in the enstrophy evolution equation; production, diffusion and dissipation terms in the presence of: (a) glass 189 μm at $\phi_{vol} = 1.77 \times 10^{-4}$; (b) glass 396 μm at $\phi_{vol} = 1.80 \times 10^{-4}$; (c) glass 396 μm at $\phi_{vol} = 3.32 \times 10^{-4}$. The enstrophy distribution has dimensional values in $1/s^2$. The distribution of each term has values of the ratio to the left-hand side of enstrophy equation.

where the inter-particle spacing becomes narrower as shown in Figs. 9(b) and (c). It can be found from Fig. 9(c) that the enstrophy production contributes to large values of the enstrophy amongst particles.

We can, thus conclude that the dominant factor responsible for the small-scale structure of turbulence modulation is the inter-particle spacing which has been neglected in the modeling of dispersed two-phase flows. The present approach indicates that the inter-particle spacing and the directional interaction must be considered in the process of turbulence distortion by particles. It thus appears that turbulence models derived from a large-scale structure of turbulence approach do not accurately simulate turbulence modulation in the presence of particles. We thus propose an approach taking into consideration the relationship between the inter-particle spacing and the scale of turbulence (Sato and Hishida, 1996), as well as the directional non-isotropic flow structure.

4. Conclusions

A Lagrangian measurement technique has been used to investigate the distortion of turbulence in the presence of particles. The present study focused on the small-scale structure of turbulence modulation in terms of the inter-particle spacing. Two classes of particles at particle volumetric fraction up to $\phi_{\mathrm{vol}} = 3.32 \times 10^{-4}$ were employed to provide characteristic values of length ratio and distance between particles, i.e., inter-particle spacing.

Turbulence augmentation by particles greater than the Kolmogorov micro-length-scale was induced by regions of high strain rate and high vorticity along both sides the particle. An application of the RDT to dispersed two-phase turbulent flows indicated a directional interaction between the flow turbulence and particles, as the particle volumetric fraction increased.

Further insight into the small-scale structure of turbulence modulation by particles was obtained by examining the enstrophy distribution. With a decrease in inter-particle spacing, the enstrophy amongst particles increased due to enstrophy production. We thus propose an approach that considers the effect of inter-particle spacing and the directional nature of non-isotropic flow structure, in terms of turbulence modeling for dispersed two-phase flows.

Acknowledgements

The authors would like to thank undergraduate student, Mr. N. Sekiya for performing the experiments and Dr. A. Tokuhiro at Japan Nuclear Cycle Development Institute for his suggestions. The work was subsidized by the Grant-in-Aid for the Japanese Ministry of Education, Science and Culture (No. 08405019).

References

Boivin, M., Simonin, O., Squires, K.D., 1998. Direct numerical simulation of turbulence modulation by particles in isotropic turbulence. Journal of Fluid Mechanics 375, 235–263.

Crowe, C.T., 1998. On models for turbulence in fluid-particle flows. 1998 ASME Fluids Engineering Division Summer Meeting (CD-ROM).

Crowe, C.T., Gillandt, I., 1998. Turbulence modulation of fluid-particle flows – a basic approach. In: Third International Conference on Multiphase Flows (CD-ROM).

Eaton, J.K., 1994. Experiments and simulations on turbulence modification by dispersed particles. In: Kobayashi, A.S. (Ed.), Applied Mechanics Review, 47(6), Part 2, part of Mechanics USA 1994, pp. S44–S48.

Elghobashi, S.E., Truesdell, G.C., 1993. On the two-way interaction between homogeneous turbulence and dispersed solid particles. I: turbulence modification. Physics of Fluids A 5, 1790–1801.

Fleckhaus, D., Hishida, K., Maeda, M., 1987. Effect of laden solid particles on the turbulent flow structure of a round free jet. Experiments in Fluids 5, 323–333.

Gore, R.A., Crowe, C.T., 1989a. Effect of particle size on modulating turbulent intensity. International Journal of Multiphase Flow 15, 279–285.

Gore, R.A., Crowe, C.T., 1989b. Effect of particle size on modulating turbulent intensity: influence of radial location. Turbulence Modification in Dispersed Multiphase Flow, ASME-FED 80, 31–35.

Hishida, K., Sato, Y., 1999. Turbulence structure of dispersed two-phase flows (measurements by laser techniques and modeling). Multiphase Science and Technology 10, 323–346.

Kevlahan, N.K.-R., 1993. Rapid distortion of turbulent structures. Applied Scientific Research 51, 411–415.

Kulick, J.D., Fessler, J.R., Eaton, J.K., 1994. Particle response and turbulence modification in fully developed channel flow. Journal of Fluid Mechanics 277, 109–134.

Rogers, C.B., Eaton, J.K., 1991. The effect of small particles on fluid turbulence in a flat-plate, turbulent boundary layer in air. Physics of Fluids A 3, 928–937.

Sakakibara, J., Hishida, K., Maeda, M., 1993. Measurements of thermally stratified pipe flow using image-processing techniques. Experiments in Fluids 16, 82–96.

Sato, Y., Hanzawa, A., Hishida, K., Maeda, M., 1995. Interactions between particle wake and turbulence in a water channel flow (PIV) measurements an modeling for turbulence modification. In: A. Serizawa et al. (Eds.), Advances in Multiphase Flow 1995, pp. 27–40.

Sato, Y., Hayashi, I., Hishida, K., 1997. Lagrangian statistics of fluid/particle correlated motion in channel flow. In: Eleventh Symposium on Turbulent Shear Flows, vol. 3, 2411–2416.

Sato, Y., Hishida, K., 1996. Transport process of turbulence energy in particle-laden turbulent flow. International Journal of Heat and Fluid Flow 17, 202–210.

Sato, Y., Hishida, K., Maeda, M., 1996. Effect of dispersed phase on modification of turbulent flow in a wall jet. Journal of Fluid Engineering 118, 307–315.

Squires, K.D., Eaton, J.K., 1990. Particle response and turbulence modification in isotropic turbulence. Physics of Fluids A 2, 1191–1203.

Tsuji, Y., Morikawa, Y., 1982. LDV measurements of an air-solid two-phase flow in a horizontal pipe. Journal of Fluid Mechanics 120, 385–409.

Tsuji, Y., Morikawa, Y., Shiomi, H., 1984. LDV measurements of an air-solid two-phase flow in a vertical pipe. Journal of Fluid Mechanics 139, 417–434.